Effects of Cyclic Hydraulic Pressure on Osteocytes

by

Chao Liu

A thesis submitted in conformity with the requirements
for the degree of Master of Applied Science

Mechanical and Industrial Engineering
University of Toronto

Effects of Cyclic Hydraulic Pressure on Osteocytes

Chao Liu

Master of Applied Science

Mechanical and Industrial Engineering
University of Toronto

2010

Abstract

Bone changes composition and structure to adapt to its mechanical environment. Osteocytes are putative mechanosensors responsible for orchestrating the bone remodeling process. Recent *in vitro* studies showed that osteocytes could sense and respond to substrate strain and fluid shear. However the capacity of osteocytes to sense cyclic hydraulic pressure (CHP) associated with physiological mechanical loading is not well understood. In this study, osteocyte-like MLO-Y4 cells were subjected to CHP of 68 kPa at 0.5 Hz, and the effects of CHP on intracellular calcium concentration, cytoskeleton organization, mRNA expression of genes related to bone remodeling, and osteocyte apoptosis were investigated. The results indicate that osteocytes could sense CHP and respond by increased intracellular calcium concentration, altered microtubule organization, an increase in COX-2 mRNA level and RANKL/OPG mRNA ratio, and decreased apoptosis. Therefore cyclic hydraulic pressure in bone a mechanical stimulus to osteocytes and may play a role in regulating bone remodeling.

Acknowledgments

I would like to give heartfelt thanks to my supervisor, Professor Lidan You, whose encouragement, guidance and support from the initial questions to the final results enabled me to develop an understanding of the subject.

I offer my regards and gratitude to all the people who have supported me in any respect during the completion of the project.

I would also like to convey thanks to the Faculty of Mechanical and Industrial Engineering for providing the financial means and laboratory facilities.

Table of Contents

List of Figures

List of Appendices

1 Introduction

Bone disorders such as osteoporosis afflict over 2 million Canadians, and contribute to 80% of hip fractures, which costs $10 billion annually in Canada [1]. Within a year, 1 in 5 with osteoporotic fracture will die [1]. People living with bone disorders become functionally dependent, and many require long-term home care[1]. Many bone diseases, including osteoporosis, are caused by the failure of bone remodelling [2].

Bone is a living organ that is able to adapt its composition and structure in response to mechanical stimuli [3, 4]. It was believed that mechanical forces stimulate bone cells to maintain tissue homeostasis in bone. Mechanical loading induces a variety of physical signals that may stimulate cells within the bone, including tissue strain, fluid shear, and fluid pore pressure. Both strain and fluid shear have been extensively studied and shown to significantly affect bone cells *in vitro* [5-10]. There are a few studies that have investigated the effects of fluid pressure *in vivo* and in *vitro* [11-15], suggesting that fluid pressure is a potent stimulus to the bone remodeling. Macroscopically, venous stasis or applied pressurization by external loading was associated with increased bone formation [16, 17]. At the tissue level, fluid pressure causes increased calcification [18], and inhibition of resorption [19]. Therefore it has been suggested that bone remodeling depends on changes in interstitial fluid pressure [14, 20-23]. However, the cellular mechanism of bone's response to fluid pressure is poorly understood.

In this study, we investigated osteocyte response to pressure using an *in vitro* approach. It has been proposed that osteocytes are the cells that detect mechanical loading in bone [24]. Osteocytes account for 90-95% of bone cells. They are embedded in the mineralized bone matrix, forming an interconnected network [25]. Due to their unique location and abundance, osteocytes are believed to be responsible for sensing mechanical loading and orchestrating the bone remodeling process.

The fluid pressure experienced by osteocytes *in vivo* is cyclic in nature, the magnitude of which was calculated to reach a maximum to 0.27 MPa [26]. Recent studies found that the hydraulic permeability of the bone tissue was smaller than the previous model assumed, leading to an even higher estimation of the maximum physiological hydraulic pressure buildup (~5 MPa) around osteocytes [27-29]. In this study, we subjected MLO-Y4 cells, a well-established osteocyte-like cell line, to a cyclic hydraulic pressure (CHP) with a peak value of 68 kPa and 2 sec per cycle. Hydraulic pressure is defined here as the pressure in a fluid system (the lacunar-canalicular system in bone) that is being acted on by an external agent. This pressure level is consistent with a moderate physiological activity such as walking, which was calculated to induce maximum of 100 kPa on the osteocytes [26]. The frequency of 0.5 Hz was chosen to differentiate the response of osteocytes to load-induced hydraulic from cardiovascular pressure, which occurs around at 1-2 Hz. Loading frequency of 0.5 Hz has also been suggested to generate central peak in the pore fluid pressure within the osteocyte cell body [30]. This loading regimen is also consistent with previous study [23].

Selective responses of osteocytes to CHP were studied, including intracellular Ca^{2+} concentration ($[Ca_{2+}]_i$), cytoskeleton organization, mRNA expressions of cyclooxygenase-2 (COX-2), receptor activator of nuclear factor kappa B (NF-κB) ligand (RANKL), and osteoprotegerin (OPG), and apoptosis. Previous studies have found that other types of mechanical stimuli such as fluid shear stress have altered these outcome measures in bone cells. Intracellular calcium is an early second messenger that plays key roles in a number of metabolic pathways [31]. Fluctuations in $[Ca^{2+}]_i$ usually increases within seconds of mechanical stimulation on bone cells [32]. In osteocytes, cell body deformation through mechanical loading induced calcium response [33]. In this study, $[Ca^{2+}]_i$ was measured and used as a indicator of responsiveness when osteocytes were subjected to CHP.

Another early-intermediate event in cellular response to mechanical loading is the changes in cytoskeleton organization. Following mechanical stimulation, cells typically show changes in cytoskeleton organization in 15 min[34]; both actin filament [34], and microtubule [35] have been shown to be integral in mechanotransduction.

Downstream gene and protein expressions are altered hours after mechanical stimulation [23]. Fluid flow applied to MLO-Y4 cells upregulated COX-2, the gene that encodes cyclooxygenase-2, a key enzyme in the production of prostaglandin E_2 (PGE_2)[10]. Substrate stretching also upregulated COX-2 [36]. The signaling molecule PGE_2 is implicated in both modeling and remodeling of bone [37]. In addition, two key molecules have been found to mediate osteoclast activity during bone resorption: RANKL and OPG. The rate of bone resorption is dependent on the RANKL/OPG ratio [38].

Furthermore, osteocyte apoptosis is a vital regulator of bone remodeling and a critical determinant of bone strength. Osteocyte apoptosis has been suggested to signal osteoclast recruitment [39, 40]. Lack of mechanical loading has been shown to be the major factor that causes osteocyte apoptosis *in vivo* [41]. However the influence of fluid pressure on osteocyte apoptosis has not been well studied *in vitro*.

The aim of this study was to investigate the effects of CHP on osteocytes. We hypothesized that CHP is an important stimulus to osteocytes and would induce significant changes in calcium mobilization, cytoskeleton morphology, and gene expression levels for COX-2, RANKL, and OPG, and osteocyte apoptosis. The results from this study bridged a gap in the knowledge of bone remodeling due to mechanical loading. From this knowledge, new pharmaceutical agents that modulate mechanotransduction pathways and exercise regimens that enhance bone health could be developed for more effective treatments of bone diseases such as osteoporosis.

2 Literature review

2.1 Forces experienced by bone cells

To understand the mechanism by which mechanical forces affect bone cell fate and function *in vivo* requires the knowledge of the mechanical forces experienced by bone cells. In mature bone

tissue undergoing remodeling, current hypotheses suggest that interstitial fluid flow is an important link by which tissue level strain is transmitted to bone cells. The strain in bone tissue in response to mechanical loads induces the pressure gradient within interstitial fluid and induces its movement within the bone pores, from the lacunar-canalicular system where osteocytes, the putative mechanosensor cells in bone, reside to the vascular system [42] [43-46] (reviewed in [47]). Interstitial fluid flow within the lacunar-canalicular porosity has been shown experimentally through tracer studies [48-51]. Movement of the interstitial fluid within the geometry of lacunar-canalicular and haversian systems would create shear stresses on bone cells, in the range of 0 to 20 dynes/cm^2 [52, 53]. According to recent poroelastic model, the level of pressure that is need to produce this level of shear stress is around 85 kPa [54].

Hydraulic pressure at the lacunar-canalicular porosity caused by physiological loading was estimated to be 40 times that induced by blood pressure difference [55], presenting a significant stimulus to osteocytes. However, few studies have been done to study the effect of static hydraulic pressure (SHP) on bone cells. Human cells experience a small change in SHP from supine to standing position. Though this change could be considered cyclic with a 12 hour period, the duration should be long enough for cells to equilibrate. This type of loading is estimated to produce 12% of the peak applied uniform axial compressive stress at the lacunar-canalicular porosity [26]. Under physiological activities, such as walking, hydraulic compression is cyclic in nature. Oscillatory loading of bone with 0-18 MPa at 1 Hz was calculated to induce 0.27 MPa fluid pressure at the lacunar-canalicular porosity [55], indicating pressure could be a significant stimulus for bone remodeling. Recent studies found that the hydraulic permeability of the bone tissue was smaller than the previous model assumed, leading to an even higher estimation of the hydraulic pressure buildup (~5 MPa) around osteocytes[27-29]. The effects of hydraulic pressure on cells are complicated by spatial heterogeneity in local cell stiffness; for example, the cell body will may deform more than cellular processes under hydraulic loads, since the cell's body is more compliant than its processes [56]. Poroelastic cell models with idealized geometries have been developed to estimate local deformation of a cell under cyclic hydrostatic pressure [30]. However, few studies have been done to investigate only the effect of hydraulic fluid pressure force on bone cells, for which the mechanotransduction pathway and effectors are still poorly understood.

2.2 Osteocyte mechanobiology

Osteocytes are essential in normal bone remodeling. Osteocyte malfunction [57] or absence [58] in mouse models leads to bone fragility consistent with that observed in aging and osteoporosis. Specifically, while osteocyte ablation increased bone resorption in mice under physiological loading, the same mice were resistant to the disuse-induced bone loss when their hind limbs were subjected to unloading [58].

Bone resorption, one of the early events in bone remodelling, is mediated by osteoclasts. Two key molecules have been found to mediate osteoclast activity during bone resorption: receptor activator of nuclear factor kappa B (NF-κB) ligand (RANKL) and osteoprotegerin (OPG). RANKL stimulates osteoclast precursors to commit to the osteoclastic phenotype. OPG binding to RANKL blocks osteoclastogenesis, and decreases the survival of pre-existing osteoclasts. Therefore the rate of bone resorption is dependent on the RANKL/OPG ratio [38]. In a transgenic mouse model in which specifically ablation of osteocytes increased RANKL/OPG ratio in bone, suggesting osteocyte is responsible for the regulation of the RANKL/OPG ration, and consequently bone resorption [58]. In mice, fluid flow-induced shear stress caused increased RANKL/OPG ratio produced by osteocytes, followed by increased number of osteoclasts and bone resorptive activities [59].

CHP has been shown to increase osteocyte viability in calve bone explant study [60]. Bone explants were subjected to CHP with peak of 3 MPa at 0.33 Hz, with a triangle waveform for 1 h/day, starting on day 2. Bone cells were harvested on days 2, 8, 15, and 22 (n = 4). By day 8, CHP increased osteocyte viability compared to controls. In osteoblast-seeded cores, CHP loading also resulted in a trend of increased osteoblast function in the presence of osteocytes [60]. This strengthens the view that osteocytes function as mechanosensors that modulate osteoblast activity. Increased proliferation was observed in rat bone marrow-derived osteoblast-like cells under CHP (0.3 – 5.0 MPa at 1 Hz) [61]. These cells were from young (12 day old) and old (1 year old) rats, and were seeded onto 3D titanium-mesh scaffold.

In contrast to enhanced viability after stimulation with mechanical loading, osteocyte apoptosis has been linked with increased bone resorption in vivo following ovariectomy [62]. It has also been shown that osteocyte apoptosis controls activation of intracortical resorption in the case of bone fatigue [63]. Therefore osteocyte apoptosis may also be a potent regulator of bone remodeling.

These observations suggest that osteocytes sense mechanical stimuli applied to the skeleton and regulate load-induced remodeling responses, an ideal role for them due to their abundance and location. Another area of significant interest is the investigation of the mechanisms by which osteocytes communicate with effector cells such as osteoclasts, osteoblasts, and their precursors to regulate bone remodeling. The possible cellular structures that are responsible for sensing mechanical force and involved in intra- or intercellular signaling are reviewed below.

2.3 Possible mechanoreceptors

2.3.1 Ion channels and cell membrane

Bone cells express stretch-activated trans-membrane ion channels. The TREK family potassium channels, which are activated by stretch and involved in loading induced up-regulation of PTH-related protein (PTHrP), were identified in osteoblast-like cells [64]. Stretching UMR201-10B osteoblast-like cells by swelling in hypotonic solutions increased PTHrP mRNA. Also PTHrP mRNA level increased in UMR-201-10B cells (2 fold) and MLO-A5 cells (3 fold) following mechanical stretch. Though receptors for sensing pressure have not been described for osteocytes, parallels have been found in other cells. The mechanosensitive channel large conductance responds to hyperosmotic tension in E. coli [65]. Cystic fibrosis transmembrane conductance regulator (CFTR), an anion and intracellular ligand-gated channel, could be activated by membrane stretch induced by negative pressures as small as 5 mmHg at the cellular level in mouse epithelial cells [66]. The cell membrane has been suggested to be a mechanosensing structure as well. The fluidity of cell membrane varies in response to changes in

osmotic pressure [67]. Consequently the function of an array of membrane-bound structures such as AChR ion channel [68], LH/hCG receptors [69], and TNF receptors [70] could be affected by the change in membrane fluidity.

2.3.2 Gap junctions and hemichannels

Gap junctions and hemichannels are composed of Connexins (Cx). Cx43 has been identified and is the most abundant connexin expressed in osteocyte-like MLO-Y4 cells and primary osteocytes [71]. Gap junctions are responsible for the propagation of Ca^{2+} signaling between embedded osteocytes and osteoblasts. Using the mice model, in vivo mechanical loading on the incisors and maxillary first molar increased cx43 mRNA expression in osteoblasts and bone lining cells, but not osteocytes [72]. However Cx43 protein increased in osteoblasts and osteocyte when subjected to loading. The increase in osteocytes was highest among the cell types. Steady fluid flow with shear stress of 1.6 Pa applied for 30 minutes and 2 hours induced the rapid opening of hemichannels, which mediate the release of prostaglandin, PGE_2 in MLO-Y4 osteocyte-like cells [73]. Specifically blocking hemichannels, but not gap junctions, significantly inhibited the release of PGE_2 by steady and pulsatile fluid flow with shear stress of 0.4, 0.8, 1.6 Pa [9].

In addition to gap junctions, osteoblasts and osteocytes express functional hemichannels, which function independently of gap junctions. Using a fluorophore that is able to pass through connexons, it was shown that oscillating fluid flow producing shear stress of 2 Pa at 1Hz activated hemichannels in MLO-Y4 osteocyte-like cells but not MC3T3-E1 osteoblast-like cells [74]. This is in agreement with earlier results [75, 76]. However, apyrase blocked fluid flow-induced dye uptake in another study by Li et al. [77], which contradicted the results from Genetos et al. This discrepancy could be due to the difference in the flow regime (unidirectional vs. oscillatory), or duration of exposure.

2.3.3 Integrin

The activation of integrin signaling is a potential mechanism which allows bone cells to sense changes in their mechanical environment. In MLO-Y4 osteocyte-like cells, the transduction of mechanical signals into ERK activation, which prevents apoptosis, requires integrin engagement, intact actin filaments and microtubules, FAK, Src kinase activity, and the adaptor protein Shc [78]. β1 integrin plays an important role in skeletal health. Phillips et al. were able to generate conditional knockout mice, which were depleted of β1integrin only in cortical osteocytes [57]. Hind limb unloading induced similar response in cancellous bone of wild type and knock-out mice; but the volume, cross-sectional area, moment of inertia and bone strength were all increased in the knock-out mice. Another study pointed to the function of β1 integrin in the negative compensatory response to disuse. Subjected to hypotonic swelling, which induce membrane stretch, matrix molecules that bind the αVβ3 integrin elicited larger responses to rat osteocytes [79].

2.3.4 Cytoskeleton

The cytoskeleton is a dynamic network of polymers which equilibrium could be disrupted by mechanical force, triggering intracellular signaling pathways. Significant difference between chicken calvaria osteocytes and osteoblasts in the distribution of actin-binding protein, fimbrin, were found when they were subjected to shear stress of 1.2 Pa [80]. In osteoblasts, shear stress induced recruitment of fimbrin to the end of stress fibers. In MLO-Y4 osteocyte-like cells, the transduction of mechanical signals into ERK activation requires integrin engagement, intact actin filaments and microtubules, FAK, Src kinase activity, and the adaptor protein Shc [78]. Results from McGarry et al. [81] showed that pulsatile fluid flow-induced PGE2 response in MLO-Y4 osteocyte-like cells was inhibited by cytoskeletal disruption, whereas in MC3T3-E1 osteoblast-like cells it was enhanced. They suggested these opposite PGE2 responses were related to differences in cytoskeletal composition (osteocyte structure is dominated by actin), also may occur via cytoskeletal modulation of shear/stretch-sensitive ion channels which are dominant in osteocyte, but not osteoblast.

Interestingly Malone et al. [82] showed that, inhibition of actin polymerization did not inhibit intracellular calcium mobilization in osteoblast-like cells (MC3T3-E1) due to oscillatory fluid flow. Instead, cells with compromised actin polymerization showed higher calcium responses both in terms of average magnitude of intracellular calcium concentration and overall number of cells exhibiting an intracellular calcium response. Cells with inhibited actin polymerization exposed to 1 hour of oscillatory fluid flow exhibited an increase in release of PGE_2 compared with untreated cells. The results of this study are counterintuitive in that PGE_2 release and mobilization of intracellular calcium depends on actin deformation, rather than polymerization. Therefore actin monomers, which concentration may increase under load due to increased stress in actin filament [21], may play a role in bone cell mechanotransduction.

2.3.5 Primary cilia

The primary cilia have gained increasing attention in bone cell mechanotransduction. The PC1/PC2 complex and primary cilia are known for sensing mechanical strain and regulating differentiation in kidney epithelial cells [83]. In Pkd1 null mice, skeletal abnormalities were observed [84-86]. Recently PC1 gene was found in MC3T3-E1 osteoblast-like, and MLO-Y4 osteocyte-like cells, and inactivation of these genes produced delayed endochondral and intramembranous bone formation in mice; constitutive expression of PC1 increased Runx2 and osteoblast marker in MC3T3-E1 cells [87]. This finding suggests a possible role of cilia in anabolic signals in osteoblast and osteocytes. It was later confirmed that both MC3T3-E1 and MLO-Y4 cells possess primary cilia, which were deflected during oscillatory fluid flow and that these primary cilia are required for osteogenic and bone resorptive responses to 1 Pa oscillatory fluid flow at 1 Hz [88]. In the same study, it was shown that primary cilia translate fluid flow into cellular responses in bone cells independently of Ca^{2+} flux and stretch-activated ion channels.

2.4 Mechanochemical responses

2.4.1 Intracellular calcium ion concentration

Increase in intracellular calcium ion concentration is one of the earliest responses of bone cells to mechanical load [32]. It occurs due to both the entry of extracellular calcium and the release of intracellular calcium [89]. When rat osteocytes were subjected to membrane stretch with bound αVβ3 integrins, intracellular calcium concentration significantly increased [79]. To investigate the ability of bone cells to exchange information through gap junctions under mechanical load, osteoblast-like (MC3T3-E1) cells were seeded on coverslip with micropatterned coating to force cultured cell to assume a grid-like pattern [90]. Then one cell was mechanically stimulated using atomic force microscopy. Intracellular calcium fluctuations were first observed in a single stimulated bone cell, and then the calcium fluctuation was observed in adjacent cells in the micropatterned network.

Chicken calvaria primary osteocytes and osteoblast were subject to steady fluid flow (1.2 Pa for 2.5 min), then calcium response were measured [91]. Osteocytes were less responsive then osteoblast. But in contrast to osteoblasts, calcium responses in osteocytes were immune to Arg-Gly-Aspcontaining peptides (GRGDS) disruption of focal adhesion, most likely because osteocytes had very low expression of vinculin [91]. These results suggest that osteocytes and osteoblast sense fluid flow-induced shear stress through different mechanoreceptors.

2.4.2 Cytoskeleton change in response to mechanical load

In osteoblast-like (MC3T3-E1) cells, in the physiological range applied for 1 hour, steady flow induced formation of stress fibers, while oscillatory fluid flow did not [82]. However Ponik et al. [10] showed that stress fibers do form in MC3T3-E1 cells, but they need to be subjected to oscillatory fluid flow for at least 5 hours. While in osteocyte-like (MLO-Y4) cells, 24 hours of steady flow was needed to elicit stress fiber formation; after 24 hours of oscillatory fluid flow the number of dendritic processes increased [10]. Under unidirectional fluid shear stress osteocyte-

like (MLO-Y4) showed increased dendricity and elongation of dendrites that depends on E11 protein [92].

The effect of CHP and SHP on osteoblast-like cells (MG-63) has been studied by Tasevski et al.[93]. The hydrostatic pressure was varied between 0 – 0.8 MPa. The CHP was applied for 1 minute on, then 14 minutes off, for durations from 4 to 12 hours. The mRNA levels for matrix metalloproteinase-1 and -3 (MMP-1 and MMP-3) were significantly increased ($p < 0.001$) in cells exposed to CHP under serum-free conditions for 4–12 h. mRNA levels for MMP-3, but not MMP-1, were significantly enhanced in cells subjected to SHP. The changes in MMP-1 and MMP-3 may indicate extra cellular matrix (ECM) turnover, and remodeling of bone. The different responses to CHP and SHP suggest that cells have different mechanosensing pathways for CHP and SHP, some of which are responsible for detecting oscillatory patterns in pressure loading. Also the different responses may lead to bone remodeling that result in different bone structure and composition.

MLO-Y4 osteocytes showed increased force traction on beads attached to the cell body, up to 30 pN. The force was enough for the activation of integrins, suggesting a mechanical feedback loop. Experiments with an atomic force microscope have shown increased elastic modulus in osteocytes after mechanical loading [94]. This stiffening response was related to changes in material properties of the cell, suggesting that the cells actively change their cytoskeleton in response to a mechanical load.

You et al. [95] suggested that drag forces on the osteocyte pericellular matrix in response to fluid flow could be coupled to, and amplified by, the actin cytoskeleton. Tethering elements, presumably composed of integrins, connect the canalicular wall and pericellular matrix to the osteocyte cytoskeleton [96]. Reilly et al. [97] showed that degrading the pericellular matrix of osteocyte-like cells diminished the release of prostaglandins following fluid flow exposure, suggesting a role in cytoskeleton-mediated mechanotransduction.

2.4.3 Prostaglandin

Pulsatile fluid flow (0.64 Pa at 5 Hz for 10 min) enhancement of PGE2 response in MLO-Y4 osteocyte-like cells depends on an intact cytoskeleton, while PGE2 response in MC3T3-E1 osteoblast-like cells was independent of cytoskeleton [81]. Oscillatory fluid flow increases PGE_2 release in MLO-Y4 cells through ATP mediated pathway, but independent of hemichannel activation [74]. Oscillatory fluid flow also increased PGE_2 expression in osteoblast-like (MC3T3-E1) cells [88]. Also Cox-2, which involves in the production of PGE_2, was upregulated in osteoblast-like (MC3T3-E1) and osteocyte-like (MLO-Y4) cells after extended period (24 hours) of both unidirectional and steady fluid flow [10].

3 Experiment design and methodology

With the resources and timeframe available for this study, the scope of the study was determined to be the investigation of the responses of osteocytes to cyclic hydraulic pressure (CHP). Specifically, seven cellular responses were measured: (1) intracellular calcium concentration, (2) actin filament and (3) microtubule network morphology, mRNA expression levels for genes (4) COX-2, (5) RANKL, and (6) OPG, and (7) osteocyte apoptosis. Cyclic hydraulic pressure with peak magnitude of 68 kPa at 0.5 Hz was chosen based on estimation from mathematical modeling and tissue level studies. The duration of CHP was determined based on the known response time of the different cellular responses. The cells were cultured *in vitro* on a flat glass surface during the application of CHP.

3.1 Cell culture

MLO-Y4 osteocyte-like cells (gift from Dr. Lynda Bonewald, University of Missouri-Kansas City, Kansas City, MO, USA) were cultured in α-Modified Eagle's Medium (α-MEM, GIBCO™) supplemented with 2.5% fetal bovine serum (FBS, Hyclone), 2.5% calf serum (CS, Hyclone), and 1% penicillin and streptomycin (P/S, GIBCO™) on 100 mm petri dishes coated with type I rat tail collagen (BD Laboratory). The cells were maintained at 37 °C and 5% CO_2 in

a humidified incubator (Thermo Scientific). Cell subculture was performed when the cells reached 70% confluence. With the exception of calcium experiments, cells were seeded on type I rat tail coated glass slides (75 mm×38 mm×1 mm) 48 h prior to CHP loading at 150,000 cells per slide to ensure 70-80% confluence at the time of experiment. For the apoptosis experiment, the cells were serum starved 24 hours prior to CHP loading with α-MEM containing 0.02% FBS, 0.02% CS, and 1% P/S. For calcium experiments, MLO-Y4 cells were seeded onto non-coated glass slides (75 mm×38 mm×1 mm) using the same culturing protocols.

3.2 Cyclic hydraulic pressure loading *in vitro*

MLO-Y4 cells were seeded onto collagen-coated glass slides, which were placed in the pressure chambers and pressure gauges (Omega Inc.) were attached to monitor the pressure inside of the chamber, as described previously [23]. The glass slide with MLO-Y4 cells were placed inside of the chamber without any fixture to hold it in place. Therefore the deformation of the chamber would create stress on the glass slide. Fresh culture media was used in the experiments for cytoskeleton staining, PGE_2 assay, and quantitative RT-PCR assays. A syringe (KD Scientific), driven by a syringe pump (Cole-Parmer), applies the hydraulic pressure loading directly to the medium filled in the pressure chamber (Figure 1). The cells were subjected to cyclic hydraulic pressure with 0.5 Hz triangular waveform which has peak pressure of 68 kPa for one or two hours. The loading regime used in this study was within the range of pressures used in other studies [17, 23, 26, 60, 89, 98-100]. Due to the relative incompressibility of the aqueous medium, a very small volume change (< 0.5 mL) was used to induce the desired pressure. This small volume was found to result in a negligible shear stress. The peak shear stress was estimated to be 4.9×10^{-3} Pa, using equation $T = 6\mu Q/(bh^2)$, where T is the shear stress; μ is the viscosity of the medium, which is approximated to be that of the water at room temperature (1×10^{-3} Pa·s); Q is the flow rate, which is 0.5 ml/s as a result of the syringe displacement; b is the flow channel width, which is 38 mm; h is the flow channel height, which is 4 mm. The calculated maximum shear stress level experienced by the cells was at least 2 orders of magnitude lower than those that are known to excite bone cells *in vitro* [101]. Therefore, the responses observed in the present study were attributed to the hydraulic pressure.

As control, collagen-coated glass slides seeded with MLO-Y4 cells were placed in pressure chambers but without application of CHP. The pressure experiments were performed at room temperature.

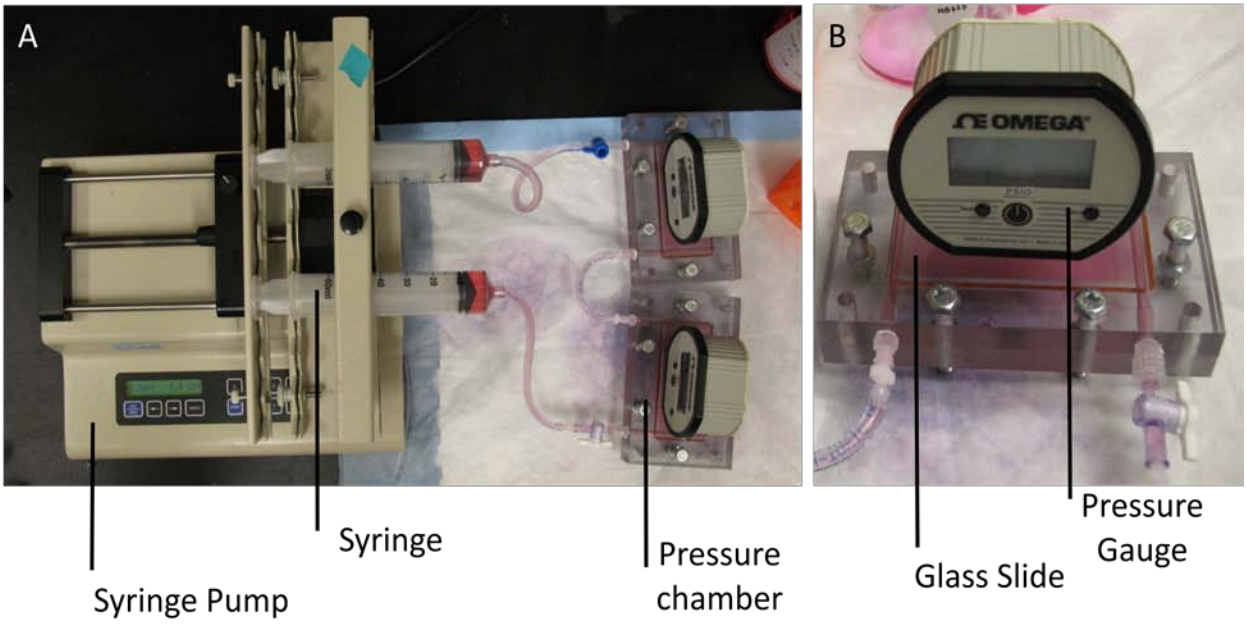

Figure 1. The system that applies cyclic hydraulic pressure consists of (A) a syringe pump driving two syringes, which are connected to two pressure chambers with pressure gauges attached. The cells, which are attached onto a glass slide, are located in the interior of the chamber (B). The pressure inside of the chamber was monitored with the pressure gauge.

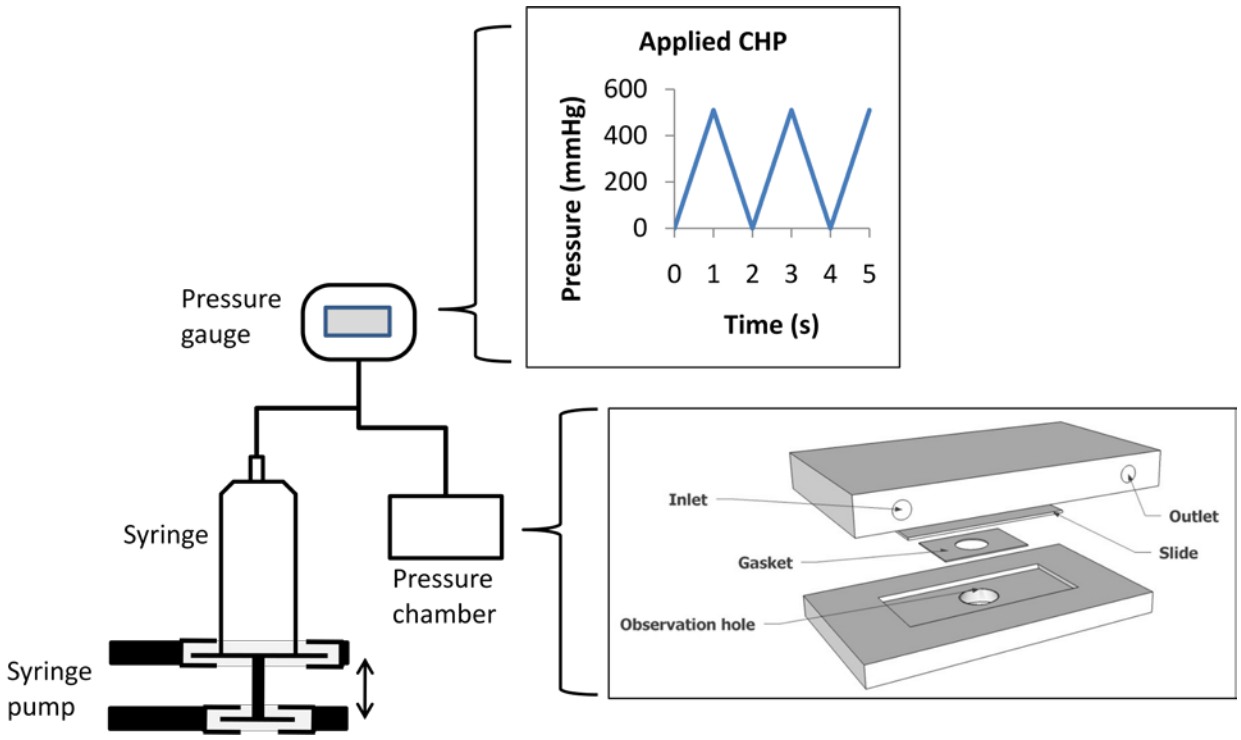

Figure 2. A syringe driven by a programmable pressure pump was used to apply CHP (0 to 68 kPa, at 0.5 Hz) to cells. The pressure inside the chamber was continuously monitored through a pressure gauge to ensure that the desired loading profile was applied. A slightly modified pressure chamber was used for real-time intracellular [Ca^{2+}] observation. The top and bottom halves of the chamber were secured with screws. The gasket, sealed with vacuum grease, prevents leakage of media inside the chamber. The microscope objectives were able to focus on the glass slide through the observation hole.

3.3 Real-time intracellular calcium measurement

Intracellular calcium ion concentration was quantified as previously described [102]. Briefly, prior to exposure to CHP, MLO-Y4 cells on quartz slides were incubated with 10 μM Fura- 2 AM (Molecular Probes, Eugene OR) for 30 min at 31 ^{0}C (to reduce dye compartmentalization), then washed with fresh working medium (α-MEM without phenol-red (GIBCO™) supplemented with 1% FBS and 1% CS). The slides were placed into a custom-made pressure chamber (Figure 2), and fixed to a pre-heated stage (31 ^{0}C) on an inverted microscope (Eclipse Ti-S, Nikon, Japan) with a calcium imaging system (PTI EasyRatioPro system, USA). For 30 min, the cells

were left undisturbed. Fresh working medium was used during the pressure experiment. During the application of pressure loading, Fura-2 340 nm/380 nm ratio values were converted to $[Ca^{2+}]_i$ values using image analysis software (EasyRatio, PTI). Baseline $[Ca^{2+}]_i$ level was recorded for three minutes, followed by application of CHP for 3 min. Images were recorded at a rate of one every 160 ms (n = 30). Temporal profiles were determined for approximately 30 cells per field of view. Each cell was classified as responding or not responding: a responding cell was defined as having at least a two fold increase in the maximum oscillation magnitude of $[Ca^{2+}]_i$ during the application CHP over the maximum oscillation recorded during the 3 min baseline period.

3.4 Cytoskeleton immunostaining and quantification

MLO-Y4 cells were exposed to CHP loading or non-loading (static control) for 1 hour, and then their actin filament and microtubules staining were performed as previously described [23] (n = 8). To stain the actin filaments, the cells were fixed with 3.7% Formaldehyde in PBS for 10 minutes, then permeabilized with 0.1% Triton X-100 in PBS for 5 minutes. The cells were stained with Alexa Fluor 488 phalloidin (Molecular Probes A-12379). To stain the microtubules, the cells were fixed with 0.25% glutaraldehyde and permeabilized with 0.1% Triton X-100 in PHEM buffer (25 mM HEPES, 60 mM PIPES, 10 mM EGTA, 2 mM MgCl, pH 6.9, warmed to 37°C) for 30 minutes. Following fixation, cells were quenched in 2 μg/ml of sodium borohydride for 15 minutes. The fixed cells were treated with 10% BSA for 1 hour to reduce non-specific binding. Microtubules were first labeled with 2 μg/ml alpha-tubulin antibody (AB Cam, Cambridge, MA, USA) for 3 hours, and then with 50 μg/ml FITC secondary antibody (Invitrogen) for 1 hour. Cells were then imaged using a laser scanning confocal microscope (Olympus, USA).

The local bending sections with high curvature in microtubule have been shown to be the result of localized buckling [103]. In this thesis, the local bending sections with high curvature in microtubules will be referred to as buckling regions. The buckling regions in microtubules were quantified using a chord-to-point distance accumulation (CPDA) method [104], implemented in MatLab. The CPDA program recognizes microtubules and calculates the number of buckling

regions and the curvatures of these buckling regions. A square ROI of 150×150 pixels was selected on the microtubule immunofluorescent images of the cell, which covers around 30% of the cell area. The ROI was selected to exclude the cell nucleus, but may include regions outside of the cell body (which will be black). The number of buckling regions and the curvature normalized with the number of buckling regions were quantified. The buckling regions in the ROI were counted and the curvature at each buckling region was calculated.

3.5 mRNA Quantification

Immediately after CHP loading, both of the loaded and control MLO-Y4 cells on glass slides were trypsinized. The total RNA was extracted from cells (n= 12) using RNeasy Mini Kit (Qiagen, USA). The extracted RNA was treated with DNase I (Fermentas) and reverse-transcribed using SuperScript^{TM} III RT (Invitrogen, USA) to synthesize cDNA. For genes COX-2, RANKL, OGP, and 18S, Quantitative PCR (qPCR) was used to amplify the cDNA of the samples using gene-specific primers and SYBR Green I (Roche, USA) in Mastercyler ep Realplex^{2} (Eppendorf, USA). The copy number of COX-2, RANKL, and OPG for each experimental group were normalized to its 18S (housekeeping gene) rRNA levels and the control group. To define the time courses of the gene expressions, the duration of the CHP stimulation was varied at one or two hours.

3.6 Apoptosis staining and quantification

To assess the effects of CHP on osteocyte apoptosis, apoptosis in MLO-Y4 cells was induced by serum starvation of the cells with α-MEM containing 0.02% FBS, 0.02% CS and 1% P/S for 24 hour prior to the application of CHP. CHP was applied for 1 hour to these serum starved MLO-Y4 cells, during which cells were exposed to fresh complete medium. Then they were incubated for 1 hour at 37 °C and 5% CO2 with fresh complete medium. The percentage of apoptotic cells was measured at prior to CHP loading (24 hours after the start of serum starvation), and compared against cells that were exposed to complete media. Apoptosis was measured again immediately after CHP (25 hour post the beginning of serum starvation) or with 1 more hour of incubation in fresh complete medium (26 hour post the beginning of serum starvation) and

compared with non-loaded controls (cells in pressure chambers without pressure loading application) (n = 8). The APOPercentage dye (Biocolor Ltd.) was used to stain the apoptotic cells. The APOPercentage dye can only be actively transported into the cells that lose their membrane asymmetry, which occurs early during apoptosis [105]. The accumulation of APOPercentage dye stains the apoptotic cells pink, allowing detection of apoptosis using a microscope. PAP pen (Sigma) was used to draw a containment oval on slides of cells subjected to either CHP or static controls. The hydrophobic ovals served as a barrier to control the staining area during the 30 minute staining process. The dye stock solution was diluted (1:20) in complete medium, and the diluted dye (50µL) was applied inside the oval barrier region. After the 30 minute incubation, the dye was removed. The region was then rinsed twice with 1mL of PBS. The cells were immersed in PBS before being photographed under a microscope. Five regions within the oval region were photographed. The cells in these photos were quantified for the number of apoptotic cells over the total number of cells in each field of view (FOV). All cells were counted using the ImageJ software with the cell counter plug-in.

3.7 Statistical Analysis

Student t-tests (performed with SPSS software) were used to determine significant differences between CHP loaded groups and static groups (control). Statistical significance was defined as $P < 0.05$ (two tailed). The error bars shown in graphs are standard deviations.

4 Results

4.1 Increased oscillations of intracellular calcium concentration

The increase in $[Ca^{2+}]_i$ during application of CHP loading was observed 40 seconds after the start of the loading (Figure 3A). Few cells showed increases in $[Ca^{2+}]_i$. during the baseline period. Upon the application of CHP, a significantly ($P = 0.002$) higher percentage of cells (20.9%) showed over two-fold increase in $[Ca^{2+}]_i$ (Figure 3B). Oscillations in $[Ca^{2+}]_i$ were observed in all cells even after the CHP loading was stopped.

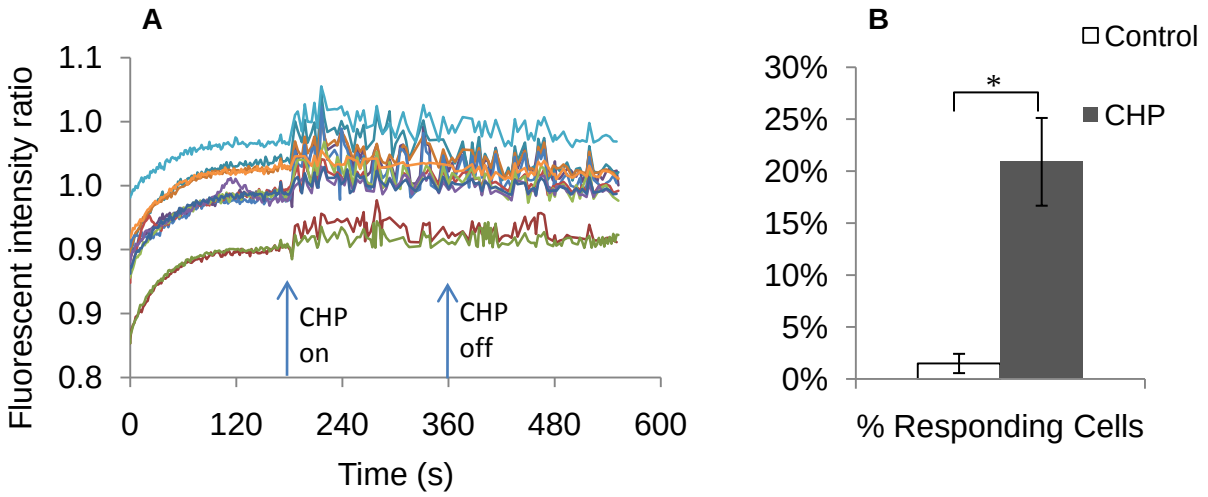

Figure 3. (A) The observed 340/380 nm fluorescent intensity ratio in representative cells. Before the application of pressure, 180 s of baseline was recorded. CHP was applied at the 180 s mark. Fluorescent intensity ratio level, which corresponds to intracellular [Ca2+], showed first peak at 36 s after the start of CHP application. (B) Effect of CHP on intracellular [Ca2+] in MLO-Y4 cells (n = 30). Significantly (P = 0.002) more cells showed more than two-fold increase in intracellular [Ca2+] when treated with CHP compared with non-loaded cell (control).

4.2 Altered microtubule morphology but with no changes in actin filament

Fluorescent staining using Alexa Fluor 488 phalloidin for actin filament showed no significant difference between MLO-Y4 cells that were subjected to CHP versus non-loaded controls (Figure 4A). No obvious stress fiber formation was observed. However, after applying CHP to MLO-Y4 cells, the microtubules showed increased buckled structure (Figure 4A). The number of buckling regions and the curvatures of these regions were computed using the CPDA algorithm implemented in MatLab. There was a 4.4-fold increase in the normalized curvatures of microtubule buckling regions (P = 0.049) (Figure 4D). However the number of detected corners, which corresponds to the number of buckling points in the microtubules, remained the same for both groups (Figure 4C).

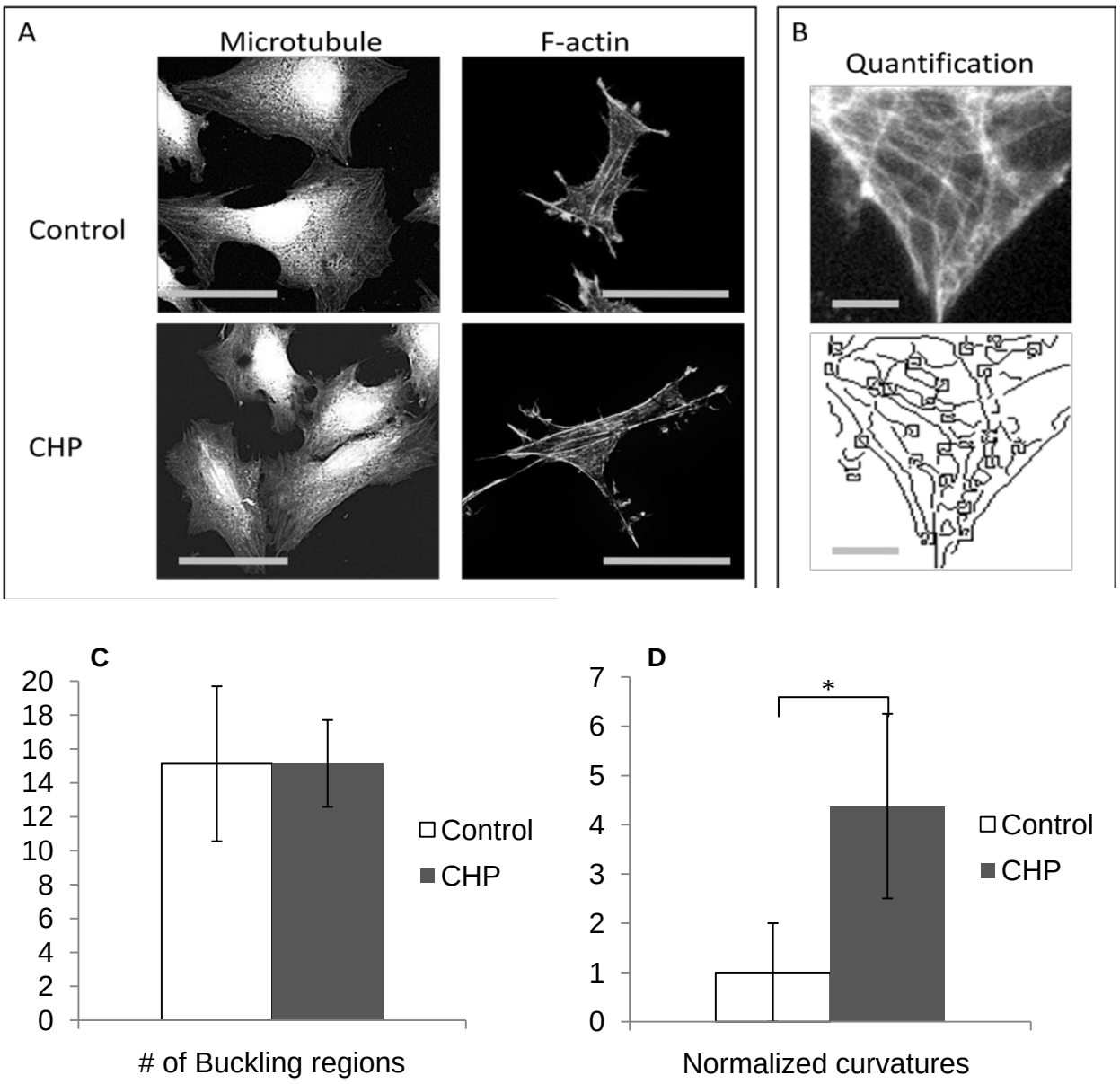

Figure 4. (A) Effect of CHP (68 kPa at 0.5 Hz for 1 hr, n = 8) on the actin filament and microtubule morphology in MLO-Y4 cells (bar = 30 μm). The microtubules showed more bended structures after the application of CHP, while the actin filament organization remained the same between the control and CHP treated groups. (B) An example of the CPDA analysis is shown (bar = 10 μm). The ROI (top panel) consists of an area of 150×150 pixel (38.8×38.8 μm). A MatLab program implementing the CPDA algorithm was used to find the buckling regions and the curvature of each buckling region (bottom panel of B). (C, D) Quantification of microtubule buckling regions after 1 hr CHP loading on MLO-Y4 cells (n = 8). (C) No significant difference

was observed in the number of microtubule buckling regions. (D) The curvature in each of the buckling regions was calculated and normalized to the no pressure condition (control).The cells treated with CHP showed significantly larger curvature compared with non-treated cells (control) ($P = 0.049$).

4.3 Increased COX-2 expression

The relative mRNA expression level of COX-2, of which presence is vital for the synthesis of PGE_2 in the cell, was measured [106-108]. Following the loading regime of 68 kPa at 0.5 Hz for 1 hr, COX-2 mRNA expression level increased by 65% in CHP loaded cells ($P = 0.006$), compared with non-loaded controls (Figure 5A). However the elevated COX-2 level was abolished after 2 hrs of CHP (68 kPa, 0.5 Hz) loading. There was no significant difference in COX-2 gene expression between the CHP and control groups after 2 hrs of loading.

4.4 RANKL/OPG expression

Opposite to the case of COX-2, the mRNA expression levels of OPG and RANKL did not show any significant change in MLO-Y4 cells and the RANKL/OPG ratio showed a slight but not statistically significant decrease after 1 hour of CHP loading (68 kPa, 0.5 Hz) (Figure 5B). Increasing the duration of the CHP loading to 2 hours, the expression levels of RANK still did not show any significant difference from the controls. However, the prolonged stimulation did result in a significant decrease (35%, $P = 0.001$) in the OPG mRNA level, and a significant increase in the RANKL/OPG ratio (60%, $P = 0.02$) (Figure 5C).

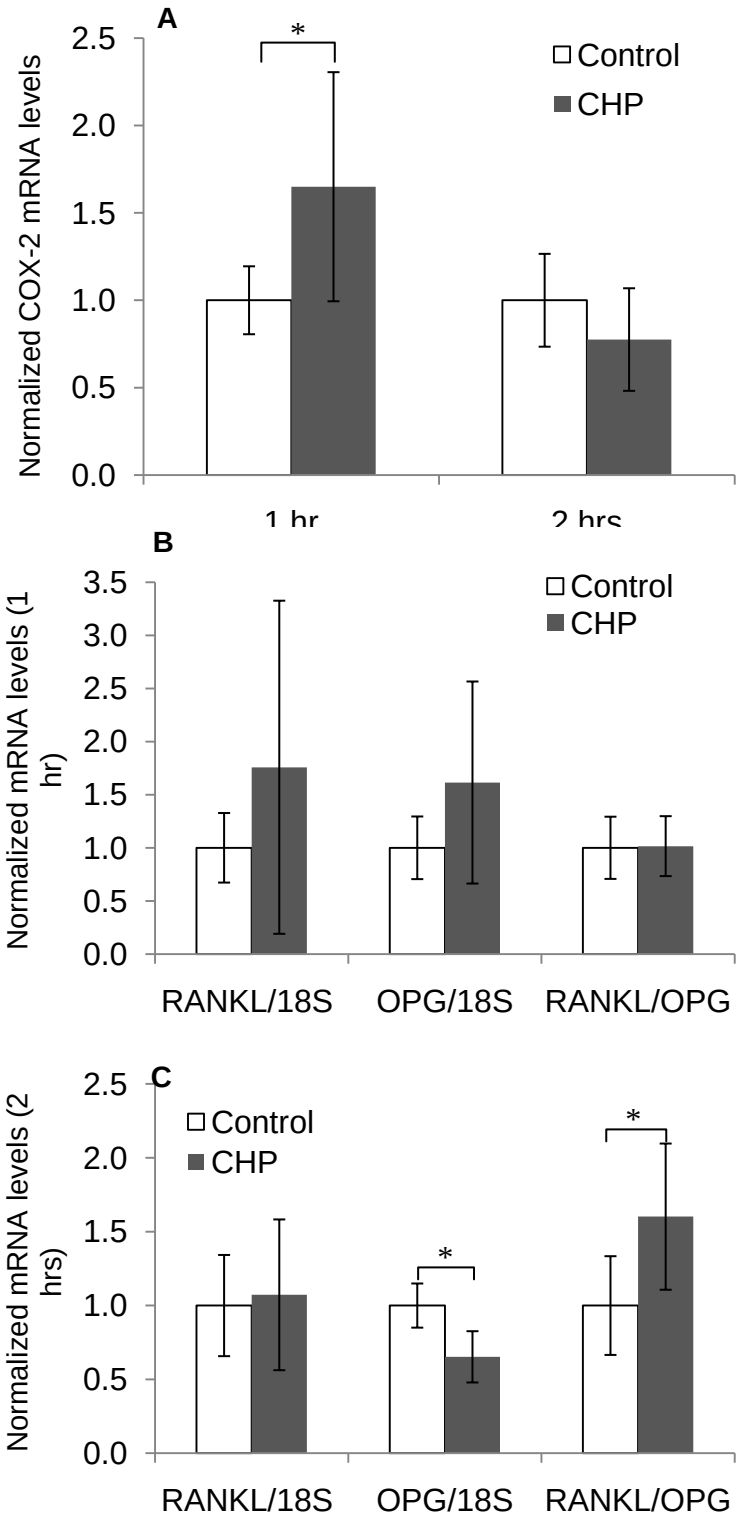

Figure 5. (A) Relative mRNA levels of COX-2 (n = 12). After 1 hr of CHP (68 kPa, 0.5 Hz) the relative expression of COX-2 mRNA in cells subjected to CHP was 1.75 times higher than that in non-loaded controls (P = 0.006). However this difference disappeared after 2 hrs of CHP. (B, C) Relative mRNA levels of OPG, RANKL and RANKL/OPG in MLO-Y4 cells (n = 12) after 1 hr (B) and 2 hrs (C) of CHP loading (68 kPa, 0.5 Hz). Sham loaded glass slides seeded with MLO-Y4 cells were used as no pressure control. No significant difference was observed in OGP, RANKL expression level, or RANKL/OPG ratios after 1 hr of CHP (B). However the OPG expression level decreased by 35% (P = 0.001), and caused the RANKL/OPG ratio in CHP treated cells increased by 82% after 2 hrs compared to the controls (P = 0.02).

4.5 Decreased osteocyte apoptosis

After 24 hours of serum starvation, the percentage of apoptotic cells was 26.5%, compared with 11.8% of cells cultured with complete medium for the same duration (P = 0.047) (Figure 6A). To determine whether CHP can inhibit the osteocyte apoptosis induced by serum starvation, we applied 1 hr CHP on MLO-Y4 cells after 24 hr serum starvation. The control group was serum starved for 24 hours and then placed in the pressure chamber for 1 hour without pressure loading. At the beginning of this one hour post serum starvation, fresh complete medium was provided to both CHP and control groups. We found that immediately after applying CHP for 1 hour (25 hours from the start of serum starvation), the percentages of apoptotic cells were not significantly different from those of non-loaded groups (Figure 6B). However, after an addition 1 hour incubation (26 hours from the start of serum starvation), there was a 50% decrease in the percentage of apoptotic cells (P = 0.006) in the CHP loaded (4.7%) compared with the control (9.3%) groups (Figure 6B). The percentage of apoptotic cells in the control groups did not change significantly after 1 hour of incubation. However, one hour incubation following the CHP treatments resulted in a significant (19%) reduction in apoptotic cells (P = 0.01) compare with CHP treatment alone. Both CHP loaded and control groups show significant decreases in percent of apoptotic cells at 26 hours after the start of serum starvation (Figure 6).

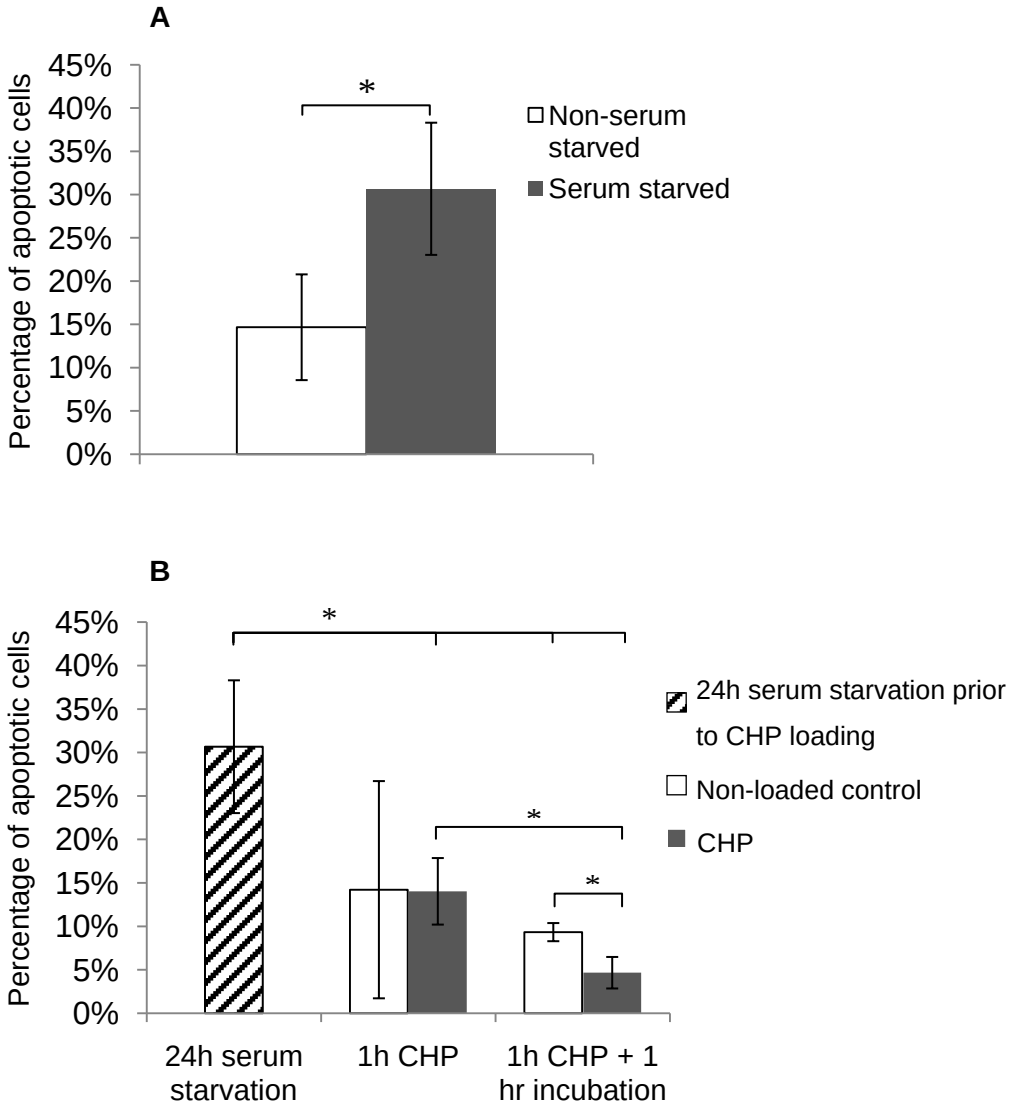

Figure 6. (A) The percentage of apoptotic MLO-Y4 cells after 24 hrs of serum starvation, compared with cells under normal conditions (n = 6, P = 0.08). (B) The percentage of apoptotic MLO-Y4 cells after 1 hr of CHP (n = 8) and with 1 additional hour of incubation. In both CHP and control groups, the percentage of apoptotic cells significantly decreased after 1hr CHP + 1hr of incubation compared with the percentage of apoptotic cells after 24 hrs of serum starvation (P = 0.0022 for Control, P = 0.0010 for CHP).The percentage of apoptotic cells between CHP and control was not significantly different immediately after 1 hr of CHP. But after an additional 1 hr incubation, the CHP treated groups (4.7%) had significantly (P = 0.006) less percentage of apoptotic cells compared to control groups (9.3%). Also, compared with cells at 25 hrs, the cells

subjected to CHP had lower percentage of apoptotic cells with 1 more hour of incubation ($P = 0.011$).

5 Discussions

Mechanical loading produces multiple physical signals that may stimulate bone cells and eventually lead to bone adaptation and remodeling. Cellular responses to some of the stimuli such as fluid shear stress and substrate stretching are relatively well studied. One of the knowledge gaps is whether osteocytes sense cyclic hydraulic pressure. In this study, we investigated the responses of osteocytes to cyclic hydraulic pressure (CHP) associated with in vivo functional loading. In specific, we showed an increase in $[Ca^{2+}]_i$ of MLO-Y4 osteocyte-like cells in response to CHP. The buckling in the osteocyte microtubules showed increased curvature after CHP loading. At the mRNA level, COX-2 expression increased after 1 hour of CHP loading; RANKL/OPG ratio showed significant increase after 2 hours of CHP loading. Lastly, we observed a beneficial effect of CHP that reduced osteocyte apoptosis induced by serum starvation.

The increase in $[Ca^{2+}]_i$ was observed under CHP stimulation but the increase was not as rapid compared to when osteocytes were subjected to fluid flow (Figure 3A). The $[Ca^{2+}]_i$ level increased after about 40 s from the start of the loading. In contrast, bone cells responded much faster under fluid shear stress stimulation, with increased $[Ca^{2+}]_i$ after about 20 seconds of loading [91]. According to the most recent poroelastic model [54], the pressure level of 68 kPa chosen in this study would elicit fluid shear stress of 1-2 Pa around the osteocytes, which covers the shear stress level used in [91]. This observation suggests that osteocytes may have a different mechanism of sensing hydraulic pressure; or the effect of CHP takes more time to develop in osteocytes. Compared with the mostly single peak response of fluid shear treated cells [91], CHP treated MLO-Y4 cells from the present study had a longer, oscillatory response. It is not clear what is the upstream event triggering this elevated $[Ca^{2+}]_I$ response. It has been shown that transient receptor potential (TRP) channels can by activated by hypo-osmotic stimulation and induce calcium ion influx in osteoblasts [109]. It is possible that similar mechanism exists in

osteocyte as well, which is responsible for the observed increase in $[Ca^{2+}]_I$ in our study. Being an early secondary messenger, increase in $[Ca^{2+}]_i$ could set off an array of downstream biochemical responses in bone cells, including autocrine and paracrine signaling [102, 110]. The increase in $[Ca^{2+}]_i$ has been found to cause translocation of nuclear factor κB to the nucleus and stimulate COX-2 expression in osteoblasts [111]. Therefore it is possible that $[Ca^{2+}]_i$ could be the cause of the elevated COX-2 mRNA expression observed in this study. It is also identified that increase in $[Ca^{2+}]_i$ could activate ERK and p38 MAPK in osteoblast [110]. It might be possible that ERK and p38 MAPK is activated by elevated $[Ca^{2+}]_i$, and this may have caused the observed increase in COX-2 expression in our study as well. There is also evidence that $[Ca^{2+}]_i$ could modulate microtubule morphology [112]. It is possible that the loading induced $[Ca^{2+}]_i$ release and changes in microtubule morphology could form a positive feedback loop that reinforces the responses of osteocytes to CHP.

The actin filament organization did not change after application of CHP, in contrast to the stress fiber formation after fluid flow [10]. However, we demonstrated that cyclic pressure loading at 68 kPa at 0.5 Hz was able to cause changes in the microtubule organization in MLO-Y4 osteocyte-like cells. In cells without external loading, microtubules have been shown to be in the state of constrained buckling with multiple buckling regions with straight segments in between [103]. From the present study, the curvatures of the bending sections in the microtubules showed significant increase in cells subjected to CHP, indicating that the buckling sections of the microtubules became more ‘compressed’ after CHP loading. Interestingly, the number of detected corners, which corresponds to buckling sections, did not increase. Several factors could contribute to this observed change in the microtubule morphology as follows: 1) Since very high pressure (100 MPa) was needed to denature proteins [113], it is more likely that the change in microtubule is a regulatory response of the cells. Calcium, which showed increased intracellular concentration in our study, has been shown to promote microtubule depolymerization [114]. 2) The change in microtubule morphology could be also related to the PGE_2 level. It has been shown that microtubule is an integral part for PGE_2 release in osteocytes [81]. 3) Changes in cytoplasmic streaming may also change the dynamics of the microtubule network, since it was shown to be affected by fluid pressure [115]. 4) The cell membrane is an often overlooked cell structure that may sense pressure loading in cells. Pressure could change the fluidity of the lipid

bi-layer [67], which would affect membrane-bound receptors [68-70]. Further studies are warranted to elucidate the molecular mechanisms of the osteocyte responses to CHP.

We showed that COX-2 expression increased after applying CHP loading to MLO-Y4 cells for 1 hour (Figure 5A). It is in agreement with a previous study in which the effects of CHP on osteoblast-like (MC3T3-E1) cells were studied [23]. The increase in COX-2 may suggest increased level of PGE_2 and its release into extracellular space, which may produce autocrine effects to i) enhance osteocyte response to mechanical loading [116], and ii) enhance osteoblast differentiation [117], leading to increased bone formation [118-120]. It has also been shown to mediate resorption [121]. In our study, the increase in COX-2 disappeared after 2 hours of CHP. This result is actually in agreement with the response induced by substrate stretching, which showed a biphasic temporal profile of COX-2 response [36]. Our study showed that COX-2 may be a part of a pathway that can be activated by all three types of mechanical loading (fluid shear stress, substrate stretching and fluid pressure), which may include adenylate cyclases, GTPase, ERK and PKA activation [122].

Both primary osteocytes and MLO-Y4 osteocyte-like cells have been shown to express RANKL and OPG, and were able to modulate osteoclast formation and activation [123]. RANKL and OPG have also been observed to be co-localized with osteocytes *in vivo* [124]. The present study showed that RANKL/OPG ratio did not change after 1 hour of CHP loading, but it increased significantly after 2 hours of CHP loading. The increase in the RANKL/OPG ratio mainly results from the decrease in OPG expression (Figure 5C). The canonical Wnt signaling, which regulates OPG expression in osteoblasts [125], might be activated by CHP. Since evidence has shown that osteocyte alone can trigger osteoclast formation [123], the results from this study indicated that long-term CHP of 68kPa level might trigger bone resorption. In contrast, 1 Pa fluid shear stress was shown to induce increases in both RANKL and OPG mRNA and protein expression, and caused the RANKL/OPG ratio to decrease [6, 59]. The magnitude of shear stress correlates to the lower end of the range that could be induced by the pressure level chose in this study. This suggest that CHP may modulate osteoclast functions in a manner different from fluid shear. Alternatively, there could be a threshold past which osteocyte would initiate bone remodeling by

up-regulating osteoclast activity. But below this threshold, the reduced RANKL/OPG ratio would down-regulate osteoclast activity and bone remodeling.

Similar to the effect of fluid shear stress [126] and substrate stretching [78] on osteocytes, CHP reduced apoptosis [60]. We have shown here that 1 hour of CHP loading was sufficient to produce anti-apoptotic effects, although the reduction in apoptotic cells was detected after 1 hour of incubation post application of CHP (Figure 6B). In our study, exposure to fresh complete medium significantly reduced the percent of apoptotic cells in both CHP and control groups, but CHP loading had a significant more reduction than the non-loaded control. Since the disruption of the asymmetric composition of cell membrane detected by the Apopercentage assay is an early event in the apoptosis process[105], it was likely that a portion of the apoptotic cells was later rescued from apoptosis by CHP. The elevated COX-2 level induced by CHP may have been beneficial for osteocyte viability [116] through Wnt/β-catenin signaling pathway[127]. Our result is consistent with previous studies with bone explants, which showed cyclic hydraulic pressure reduced osteocyte apoptosis [60]. Also based on the results from the current study, it is also possible that cells sense changes in hydraulic pressure through altered polymerization dynamics of the microtubules. Reduce number and/or length of microtubules could increase the load on the microtubule, causing increased curvature in the buckling regions.

The system to apply cyclic hydraulic pressure developed for this study fulfilled the requirement to provide physiological level of pressure and frequency *in vitro*. It also effectively eliminated the effect contributed by fluid flow. This system also eliminated the complication of changing partial pressure of dissolved gases due to a gas-liquid interface, which exists in other systems [101]. This system also allows quick assembly and recovery of cells and conditioned media. However, this system is not without drawbacks. The lack of the media perfusion system to feed fresh media into the chambers could lead to hypoxia of the cells in experiment lasting days to weeks. Due to the limitations of the syringe pump, hydraulic pressure of higher than 100 kPa or frequency of over 1 Hz could not be applied reliably in this study. Studying the cells' response to higher pressure levels and frequencies may reveal further knowledge of the cellular mechanisms of bone remodeling. Future studies in this area could use a low speed perfusion system to introduce fresh, oxygenated media to the cells. The speed of perfusion needs to be calibrated to

avoid fluid flow related stimulation of the cells. High pressure syringe pump could be used to drive more robust syringes to achieve higher pressure and frequency.

Many effects of cyclic hydraulic pressure on osteocytes have been identified and measured in this study. However, the mechanism by which the cells sense hydraulic pressure is still far from clear, not only for bone cells but cell in general. Though not in the scope of the current study, understanding the sensory mechanism in cells will aid in the investigation of bone remodeling. In fibroblasts, β_1- integrin has been shown to mediate cell response to hydraulic pressure [128] by altered binding affinity through phosphorylation of beta1-integrin at threonine 788/789 [129]. Interestingly, β_1- integrin expressed by cortical osteocytes has also been shown to be an important factor in load-induced bone formation [130]. Taken together, these studies hint that β_1-integrin maybe a good starting point when investigating the pressure sensing mechanism in osteocytes.

The cellular responses measured in this study are but a small set of the total response of osteocytes to cyclic hydraulic pressure. There are many other signaling pathways and related cytokines that regulate bone remodeling. Sclerostin is a negative regulator of bone formation [131], which is partly controlled by the Wnt signaling pathway, is sensitive to mechanical stimulus *in vivo* [8]. The Wnt signaling pathway and its related ERK signaling have been shown to also play a role in the mechanotransduction of pressure loading in mesenchymal stem cells [132]. These may be starting point for future studies into the responses of osteocytes to hydraulic pressure loading. Also, microarray analysis could screen a large number of genes to obtain a complete picture of osteocyte response to pressure loading.

The effector cells in bone remodeling, the osteoclasts and osteoblast, may react differently to different combinations of signaling molecules released by osteocytes. The RANKL/OPG response observed in this study indicates that osteocyte responses to fluid flow and pressure stimulus are different. In future studies, it may be useful to study the differential effect of

different kinds of mechanical loading on the effector cells through co-culture system or conditioned media experiments.

In summary, the present study found that osteocytes were able to detect and respond to cyclic hydraulic pressure *in vitro*. As tested in the present study with a cyclic pressure at 68 kPa level, 20.9% of the MLO-Y4 cells responded to the simulation by increasing the $[Ca^{2+}]_i$ 40 s after the onset of loading. The curvature of the buckling points in microtubules increased after 1 hour of pressure loading. The COX-2 mRNA level increased after 1 hour of loading and the RANKL/OPG ratio increased significantly after 2 hours (but not 1 hour) of loading. Further study is needed to elucidate the dose and frequency responses to cyclic hydraulic pressures at varied magnitudes and frequencies. Recent study suggests that the osteocytes may experience up to 5 MPa fluid pressure under 1000 microstrain loading at 1 Hz [29].

6 Conclusions

Our study suggests that CHP is a significant stimulus to osteocytes, which in turn have the capacity to direct bone remodeling. Systematic examination of the effects of CHP on osteocytes will lead toward a better understanding and consequently better controlling of bone remodeling for the treatments of bone diseases such as osteoporosis and the enhancement of bone health.

References

1. Lorrain, J., et al., Population demographics and socioeconomic impact of osteoporotic fractures in Canada. Menopause, 2003. **10**(3): p. 228-234.
2. Manolagas, S.C. and R.L. Jilka, Mechanisms of disease: Bone marrow, cytokines, and bone remodeling - Emerging insights into the pathophysiology of osteoporosis. New England Journal of Medicine, 1995. **332**(5): p. 305-311.
3. Frost, H.M., Skeletal structural adaptations to mechanical usage (SATMU): 1. Redefining Wolff's law: The bone modeling problem. Anatomical Record, 1990. **226**(4): p. 403-413.
4. Aguirre, J.I., et al., Increased prevalence of osteocyte apoptosis precedes osteoclastic bone resorption and the loss of bone mineral and strength induced by lack of mechanical forces in a murine model of unloading. Journal of bone and mineral research, 2004. **19**: p. S137-S137.
5. Riddle, R.C. and H.J. Donahue, From streaming potentials to shear stress: 25 Years of bone cell mechanotransduction. Journal of Orthopaedic Research, 2009. **27**(2): p. 143-149.
6. Kim, C.H., K.H. Kim, and C.R. Jacobs, Effects of high frequency loading on RANKL and OPG mRNA expression in ST-2 murine stromal cells. BMC Musculoskeletal Disorders, 2009. **10**(1).
7. Bonivtch, A.R., et al., Direct Correlation of Osteocyte Deformation with Calcium Influx in Response to Fluid Flow Shear Stress. Journal of bone and mineral research, 2008. **23**: p. S145-S145.
8. Robling, A.G., et al., Mechanical stimulation of bone in vivo reduces osteocyte expression of Sost/sclerostin. Journal of Biological Chemistry, 2008. **283**(9): p. 5866-5875.
9. Siller-Jackson, A.J., et al., Adaptation of connexin 43-hemichannel prostaglandin release to mechanical loading. Journal of Biological Chemistry, 2008. **283**(39): p. 26374-26382.
10. Ponik, S.M., J.W. Triplett, and F.M. Pavalko, Osteoblasts and osteocytes respond differently to oscillatory and unidirectional fluid flow profiles. Journal of Cellular Biochemistry, 2007. **100**(3): p. 794-807.
11. Bourret, L.A. and G.A. Rodan, The role of calcium in the inhibition of cAMP accumulation in epiphyseal cartilage cells exposed to physiological pressure. Journal of cellular physiology, 1976. **88**(3): p. 353-361.
12. Bagi, C. and E.H. Burger, Mechanical stimulation by intermittent compression stimulates sulfate incorporation and matrix mineralization in fetal mouse long-bone rudiments under serum-free conditions. Calcified Tissue International, 1989. **45**(6): p. 342-347.
13. Imamura, K., et al., Continuously applied compressive pressure induces bone resorption by a mechanism involving prostaglandin E2 synthesis. Journal of cellular physiology, 1990. **144**(2): p. 222-228.
14. Burger, E.H., J. Klein-Nulend, and J.P. Veldhuijzen, Mechanical stress and osteogenesis in vitro. Journal of bone and mineral research, 1992. **7**(SUPPL.).

15. Brighton, C.T., et al., The biochemical pathway mediating the proliferative response of bone cells to a mechanical stimulus. Journal of Bone and Joint Surgery - Series A, 1996. **78**(9): p. 1337-1347.

16. Kelly, P.J. and J.T. Bronk, Venous pressure and bone formation. Microvascular Research, 1990. **39**(3): p. 364-375.

17. Qin, Y.X., et al., Fluid pressure gradients, arising from oscillations in intramedullary pressure, is correlated with the formation of bone and inhibition of intracortical porosity. Journal of Biomechanics, 2003. **36**(10): p. 1427-1437.

18. Klein-Nulend, J., Increased calcification of growth plate cartilage as a result of compressive force in vitro. Arthritis and rheumatism, 1986. **29**(8): p. 1002.

19. Klein-Nulend, J., Inhibition of osteoclastic bone resorption by mechanical stimulation in vitro. Arthritis and rheumatism, 1990. **33**(1): p. 66.

20. Tanck, E., et al., Why does intermittent hydrostatic pressure enhance the mineralization process in fetal cartilage? Journal of Biomechanics, 1999. **32**(2): p. 153-161.

21. Myers, K.A., et al., Hydrostatic pressure sensation in cells: Integration into the tensegrity model. Biochemistry and cell biology, 2007. **85**(5): p. 543-551.

22. Wu, M.J., Effects of hydrostatic pressure on cytoskeleton and BMP-2, TGF-beta, SOX-9 production in rat temporomandibular synovial fibroblasts. Osteoarthritis and Cartilage, 2008. **16**(1): p. 41.

23. Gardinier, J.D., et al., Cyclic Hydraulic Pressure and Fluid Flow Differentially Modulate Cytoskeleton Re-Organization in MC3T3 Osteoblasts. Cellular and Molecular Bioengineering, 2009. **2**(1): p. 133-143.

24. Turner, C.H., et al., Mechanobiology of the skeleton. Science signaling, 2009. **2**(68).

25. Burger, E.H. and J. Klein-Nulend, Mechanotransduction in bone - Role of the lacunocanalicular network. Faseb Journal, 1999. **13**(8 SUPPL.).

26. Zhang, D., S. Weinbaum, and S.C. Cowin, Estimates of the peak pressures in bone pore water. Journal of biomechanical engineering, 1998. **120**(6): p. 697.

27. Cowin, S.C., G. Gailani, and M. Benalla, Hierarchical poroelasticity: movement of interstitial fluid between porosity levels in bones. Philosophical Transactions of the Royal Society A: Mathematical, Physical and Engineering Sciences, 2009. **367**(1902): p. 3401-3444.

28. Gailani, G.B., et al., Experimental protocol for the measurement of the permeability of a single osteon. J. Biomech. Eng., 2009. **in press**.

29. Gardinier, J.D., et al., In situ permeability measurement of the mammalian lacunar-canalicular system. Bone, 2010. **46**(4): p. 1075-1081.

30. Zhang, D., Oscillatory pressurization of an animal cell as a poroelastic spherical body. Annals of biomedical engineering, 2005. **33**(9): p. 1249.

31. Berridge, M.J., P. Lipp, and M.D. Bootman, The versatility and universality of calcium signalling. Nature Reviews Molecular Cell Biology, 2000. **1**(1): p. 11-21.

32. Hung, C.T., et al., Real-time calcium response of cultured bone cells to fluid flow. Clinical Orthopaedics and Related Research, 1995(313): p. 256-269.

33. Adachi, T., et al., Calcium response in single osteocytes to locally applied mechanical stimulus: Differences in cell process and cell body. Journal of Biomechanics, 2009. **42**(12): p. 1989-1995.

34. Myers, K.A., et al., Osteoblast-like cells and fluid flow: Cytoskeleton-dependent shear sensitivity. Biochemical and biophysical research communications, 2007. **364**(2): p. 214-219.

35. Pavalko, F.M., et al., Fluid shear-induced mechanical signaling in MC3T3-E1 osteoblasts requires cytoskeleton-integrin interactions. American Journal of Physiology- Cell Physiology, 1998. **275**(6): p. 1591-1601.

36. Kawata, A. and Y. Mikuni-Takagaki, Mechanotransduction in stretched osteocytes - temporal expression of immediate early and other genes. Biochemical and biophysical research communications, 1998. **246**(2): p. 404-408.

37. Tian, X.Y., et al., Continuous PGE2 leads to net bone loss while intermittent PGE2 leads to net bone gain in lumbar vertebral bodies of adult female rats. Bone, 2008. **42**(5): p. 914-920.

38. Boyle, W.J., W.S. Simonet, and D.L. Lacey, Osteoclast differentiation and activation. Nature, 2003. **423**(6937): p. 337-342.

39. Burger, E.H., J. Klein-Nulend, and T.H. Smit, Strain-derived canalicular fluid flow regulates osteoclast activity in a remodelling osteon - A proposal. Journal of Biomechanics, 2003. **36**(10): p. 1453-1459.

40. Aguirre, J.I., et al., Osteocyte apoptosis is induced by weightlessness in mice and precedes osteoclast recruitment and bone loss. Journal of bone and mineral research, 2006. **21**(4): p. 605-615.

41. Aguirre, J., et al., Osteocyte apoptosis and the loss of bone mineral and strength induced by tail suspension in mice is entirely caused by reduced mechanical strains, whereas osteoblast apoptosis is due to endogenous glucocorticoid actions. Journal of bone and mineral research, 2005. **20**(9): p. S24-S24.

42. Piekarski, K. and M. Munro, Transport mechanism operating between blood supply and osteocytes in long bones. Nature, 1977. **269**(5623): p. 80-82.

43. Jacobs, C.R., et al., Differential effect of steady versus oscillating flow on bone cells. J Biomech, 1998. **31**(11): p. 969-76.

44. Tan, S.D., et al., Fluid shear stress inhibits TNFalpha-induced osteocyte apoptosis. J Dent Res, 2006. **85**(10): p. 905-9.

45. You, J., et al., Substrate deformation levels associated with routine physical activity are less stimulatory to bone cells relative to loading-induced oscillatory fluid flow. J Biomech Eng, 2000. **122**(4): p. 387-93.

46. You, L., et al., Osteocytes as mechanosensors in the inhibition of bone resorption due to mechanical loading. Bone, 2008. **42**(1): p. 172-9.

47. Fritton, S.P. and S. Weinbaum, Fluid and Solute Transport in Bone: Flow-Induced Mechanotransduction. Annual Review of Fluid Mechanics, 2009. **41**: p. 347-374.

48. Knothe Tate, M.L. and U. Knothe, An ex vivo model to study transport processes and fluid flow in loaded bone. Journal of Biomechanics, 2000. **33**(2): p. 247-254.

49. Knothe Tate, M.L., et al., In vivo demonstration of load-induced fluid flow in the rat tibia and its potential implications for processes associated with functional adaptation. Journal of Experimental Biology, 2000. **203**(18): p. 2737-2745.

50. Mak, A.F.T., et al., A histomorphometric observation of flows in cortical bone under dynamic loading. Microvascular Research, 2000. **59**(2): p. 290-300.

51. Tami, A.E., M.B. Schaffler, and M.L. Knothe Tate, Probing the tissue to subcellular level structure underlying bone's molecular sieving function. Biorheology, 2003. **40**(6): p. 577-590.

52. Mi, L.Y., et al., Analysis of avian bone response to mechanical loading, Part Two: Development of a computational connected cellular network to study bone intercellular communication. Biomechanics and Modeling in Mechanobiology, 2005. **4**(2-3): p. 132-146.

53. Mi, L.Y., et al., Analysis of avian bone response to mechanical loading - Part One: Distribution of bone fluid shear stress induced by bending and axial loading. Biomechanics and Modeling in Mechanobiology, 2005. **4**(2-3): p. 118-131.

54. Goulet, G.C., et al., Poroelastic evaluation of fluid movement through the lacunocanalicular system. Annals of Biomedical Engineering, 2009. **37**(7): p. 1390-1402.

55. Zhang, D., S. Weinbaum, and S. Cowin, On the calculation of bone pore water pressure due to mechanical loading. International journal of solids and structures, 1998. **35**(34-35): p. 4981.

56. Docheva, D., et al., Researching into the cellular shape, volume and elasticity of mesenchymal stem cells, osteoblasts and osteosarcoma cells by atomic force microscopy: Stem Cells. Journal of Cellular and Molecular Medicine, 2008. **12**(2): p. 537-552.

57. Phillips, J.A., et al., Role for β1 integrins in cortical osteocytes during acute musculoskeletal disuse. Matrix Biology, 2008. **27**(7): p. 609-618.

58. Tatsumi, S., et al., Targeted Ablation of Osteocytes Induces Osteoporosis with Defective Mechanotransduction. Cell Metabolism, 2007. **5**(6): p. 464-475.

59. You, L., et al., Osteocytes as mechanosensors in the inhibition of bone resorption due to mechanical loading. Bone, 2008. **42**(1): p. 172-179.

60. Takai, E., et al., Osteocyte viability and regulation of osteoblast function in a 3D trabecular bone explant under dynamic hydrostatic pressure. Journal of bone and mineral research, 2004. **19**(9): p. 1403.

61. Walboomers, X.F., et al., Hydrodynamic compression of young and adult rat osteoblast-like cells on titanium fiber mesh. Journal of biomedical materials research. Part A, 2006. **76**(1): p. 16.

62. Emerton, K.B., et al., Osteocyte apoptosis and control of bone resorption following ovariectomy in mice. Bone. **46**(3): p. 577-583.

63. Cardoso, L., et al., Osteocyte Apoptosis Controls Activation of Intracortical Resorption in Response to Bone Fatigue. Journal of Bone and Mineral Research, 2009. **24**(4): p. 597-605.

64. Chen, X., et al., Stretch-induced PTH-related protein gene expression in osteoblasts. Journal of bone and mineral research, 2005. **20**(8): p. 1454-1461.

65. Sukharev, S.I., et al., Mechanosensitive channels of Escherichia coli: The MscL gene, protein, and activities, in Annual Review of Physiology. 1997. p. 633-657.

66. Zhang, W.K., et al., Mechanosensitive gating of CFTR. Nature Cell Biology, 2010. **12**(5): p. 507-512.

67. Haidekker, M.A., H.Y. Stevens, and J.A. Frangos, Cell membrane fluidity changes and membrane undulations observed using a laser scattering technique. Annals of Biomedical Engineering, 2004. **32**(4): p. 531-536.

68. Sunshine, C. and M.G. McNamee, Lipid modulation of nicotinic acetylcholine receptor function: The role of membrane lipid composition and fluidity. Biochimica et Biophysica Acta - Biomembranes, 1994. **1191**(1): p. 59-64.

69. Kolena, J., P. Blazicek, and S. Horkovics-Kovats, Modulation of rat testicular LH/hCG receptors by membrane lipid fluidity. Molecular and Cellular Endocrinology, 1986. **44**(1): p. 69-76.

70. Tappia, P.S., et al., The influence of membrane fluidity, TNF receptor binding, cAMP production and GTPase activity on macrophage cytokine production in rats fed a variety of fat diets. Molecular and Cellular Biochemistry, 1997. **166**(1-2): p. 135-143.

71. Kato, Y., et al., Establishment of an osteocyte-like cell line, MLO-Y4. Journal of bone and mineral research, 1997. **12**(12): p. 2014-2023.

72. Gluhak-Heinrich, J., et al., Mechanical loading stimulates expression of connexin 43 in alveolar bone cells in the tooth movement model. Cell Communication and Adhesion, 2006. **13**(1-2): p. 115-125.

73. Siller-Jackson, A.J., et al., alpha 5 integrin association with Cx43 regulates the function of osteocyte hemichannels in response to shear stress. Journal of bone and mineral research, 2007. **22**: p. S358-S358.

74. Genetos, D.C., et al., Oscillating fluid flow activation of gap junction hemichannels induces ATP release from MLO-Y4 osteocytes. Journal of cellular physiology, 2007. **212**(1): p. 207-214.

75. Jiang, J.X. and P.P. Cherian, Hemichannels formed by connexin 43 play an important role in the release of protaglandin E2 by osteocytes in response to mechanical strain. Cell Communication and Adhesion, 2003. **10**(4-6): p. 259-264.

76. Cherian, P.P., et al., Mechanical strain opens connexin 43 hemichannels in osteocytes: A novel mechanism for the release of prostaglandin. Molecular Biology of the Cell, 2005. **16**(7): p. 3100-3106.

77. Li, J., et al., The P2X7 nucleotide receptor mediates skeletal mechanotransduction. Journal of Biological Chemistry, 2005. **280**(52): p. 42952-42959.

78. Plotkin, L.I., et al., Mechanical stimulation prevents osteocyte apoptosis: requirement of integrins, Src kinases, and ERKs. American Journal of Physiology-Cell Physiology, 2005. **289**(3): p. C633-C643.

79. Miyauchi, A., et al., αvβ3 Integrin ligands enhance volume-sensitive calcium influx in mechanically stretched osteocytes. Journal of bone and mineral metabolism, 2006. **24**(6): p. 498-504.

80. Kamioka, H., et al., Terminal differentiation of osteoblasts to osteocytes is accompanied by dramatic changes in the distribution of actin-binding proteins. Journal of bone and mineral research, 2004. **19**(3): p. 471-478.

81. McGarry, J.G., J. Klein-Nulend, and P.J. Prendergast, The effect of cytoskeletal disruption on pulsatile fluid flow-induced nitric oxide and prostaglandin E2 release in osteocytes and osteoblasts. Biochemical and biophysical research communications, 2005. **330**(1): p. 341-348.

82. Malone, A.M.D., et al., The role of actin cytoskeleton in oscillatory fluid flow-induced signaling in MC3T3-E1 osteoblasts. American Journal of Physiology - Cell Physiology, 2007. **292**(5): p. C1830-C1836.

83. Nauli, S.M., et al., Polycystins 1 and 2 mediate mechanosensation in the primary cilium of kidney cells. Nature Genetics, 2003. **33**(2): p. 129-137.

84. Boulter, C., et al., Cardiovascular, skeletal, and renal defects in mice with a targeted disruption of the Pkd1 gene. Proceedings of the National Academy of Sciences of the United States of America, 2001. **98**(21): p. 12174-12179.

85. Lu, W., et al., Comparison of Pkd1-targeted mutants reveals that loss of polycystin-1 causes cystogenesis and bone defects. Human Molecular Genetics, 2001. **10**(21): p. 2385-2396.

86. Herron, B.J., et al., Efficient generation and mapping of recessive developmental mutations using ENU mutagenesis. Nature Genetics, 2002. **30**(2): p. 185-189.

87. Xiao, Z., et al., Cilia-like structures and polycystin-1 in osteoblasts/osteocytes and associated abnormalities in skeletogenesis and Runx2 expression. Journal of Biological Chemistry, 2006. **281**(41): p. 30884-30895.

88. Malone, A.M.D., et al., Primary cilia mediate mechanosensing in bone cells by a calcium-independent mechanism. Proceedings of the National Academy of Sciences of the United States of America, 2007. **104**(33): p. 13325-13330.

89. Hung, C.T., et al., Intracellular Ca2+ stores and extracellular Ca2+ are required in the real-time Ca2+ response of bone cells experiencing fluid flow. Journal of Biomechanics, 1996. **29**(11): p. 1411-1417.

90. Guo, X.E., et al., Intracellular calcium waves in bone cell networks under single cell nanoindentation. MCB Molecular and Cellular Biomechanics, 2006. **3**(3): p. 95-107.

91. Kamioka, H., et al., Fluid shear stress induces less calcium response in a single primary osteocyte than in a single osteoblast: Implication of different focal adhesion formation. Journal of bone and mineral research, 2006. **21**(7): p. 1012-1021.

92. Zhang, K., et al., E11/gp38 selective expression in osteocytes: Regulation by mechanical strain and role in dendrite elongation. Molecular and Cellular Biology, 2006. **26**(12): p. 4539-4552.

93. Tasevski, V., et al., Influence of mechanical and biological signals on gene expression in human MG-63 cells: evidence for a complex interplay between hydrostatic compression and vitamin D 3 or TGF-beta 1 on MMP-1 and MMP-3 mRNA level. Biochemistry and cell biology, 2005. **83**(1): p. 96.

94. Zhang, X., et al., Real-time observations of mechanical stimulus-induced enhancements of mechanical properties in osteoblast cells. Ultramicroscopy, 2008. **108**(10): p. 1338-1341.

95. You, L., et al., A model for strain amplification in the actin cytoskeleton of osteocytes due to fluid drag on pericellular matrix. Journal of Biomechanics, 2001. **34**(11): p. 1375-1386.

96. You, L.D., et al., Ultrastructure of the osteocyte process and its pericellular matrix. Anatomical Record Part a-Discoveries in Molecular Cellular and Evolutionary Biology, 2004. **278A**(2): p. 505-513.

97. Reilly, G.C., et al., Fluid flow induced PGE2 release by bone cells is reduced by glycocalyx degradation whereas calcium signals are not. Biorheology, 2003. **40**(6): p. 591-603.

98. Klein-Nulend, J., Mechanical stimulation of osteopontin mRNA expression and synthesis in bone cell cultures. Journal of cellular physiology, 1997. **170**(2): p. 174.

99. Nagatomi, J., et al., Frequency- and duration-dependent effects of cyclic pressure on select bone cell functions. Tissue Engineering, 2001. **7**(6): p. 717-728.

100. Roelofsen, J., Mechanical stimulation by intermittent hydrostatic compression promotes bone-specific gene expression in vitro. Journal of Biomechanics, 1995. **28**(12): p. 1493.

101. Klein-Nulend, J., et al., Sensitivity of osteocytes to biomechanical stress in vitro. FASEB Journal, 1995. **9**(5): p. 441-445.

102. Jacobs, C.R., et al., Differential effect of steady versus oscillating flow on bone cells. Journal of Biomechanics, 1998. **31**(11): p. 969-976.

103. Brangwynne, C.P., et al., Microtubules can bear enhanced compressive loads in living cells because of lateral reinforcement. Journal of Cell Biology, 2006. **173**(5): p. 733-741.

104. Awrangjeb, M. and G. Lu, Robust image corner detection based on the chord-to-point distance accumulation technique. IEEE Transactions on Multimedia, 2008. **10**(6): p. 1059-1072.

105. Zhou, Q., et al., Molecular cloning of human plasma membrane phospholipid scramblase. Journal of Biological Chemistry, 1997. **272**(29): p. 18240-18244.

106. Murakami, M., et al., Regulation of prostaglandin E2 biosynthesis by inducible membrane-associated prostaglandin E2 synthase that acts in concert with cyclooxygenase-2. Journal of Biological Chemistry, 2000. **275**(42): p. 32783-32792.

107. Langenbach, R., et al., Prostaglandin synthase 1 gene disruption in mice reduces arachidonic acid- induced inflammation and indomethacin-induced gastric ulceration. Cell, 1995. **83**(3): p. 483-492.

108. Dinchuk, J.E., et al., Renal abnormalities and an altered inflammatory response in mice lacking cyclooxygenase II. Nature, 1995. **378**(6555): p. 406-409.

109. Gomis, A., et al., Hypoosmotic- and pressure-induced membrane stretch activate TRPC5 channels. Journal of Physiology, 2008. **586**(23): p. 5633-5649.

110. You, J., et al., Osteopontin Gene Regulation by Oscillatory Fluid Flow via Intracellular Calcium Mobilization and Activation of Mitogen-activated Protein Kinase in MC3T3-E1 Osteoblasts. Journal of Biological Chemistry, 2001. **276**(16): p. 13365-13371.

111. Chen, N.X., et al., Fluid shear-induced NFÎºB translocation in osteoblasts is mediated by intracellular calcium release. Bone, 2003. **33**(3): p. 399-410.

112. Buljan, V., E.P. Ivanova, and K.M. Cullen, How calcium controls microtubule anisotropic phase formation in the presence of microtubule-associated proteins in vitro. Biochemical and biophysical research communications, 2009. **381**(2): p. 224-228.

113. Gross, M. and R. Jaenicke, Proteins under pressure. The influence of high hydrostatic pressure on structure, function and assembly of proteins and protein complexes. European Journal of Biochemistry, 1994. **221**(2): p. 617-630.

114. O'Brien, E.T., E.D. Salmon, and H.P. Erickson, How calcium causes microtubule depolymerization. Cell Motility and the Cytoskeleton, 1997. **36**(2): p. 125-135.

115. Staves, M.P., R. Wayne, and A.C. Leopold, Hydrostatic pressure mimics gravitational pressure in characean cells. Protoplasma, 1992. **168**(3-4): p. 141-152.

116. Bonewald, L.F. and M.L. Johnson, Osteocytes, mechanosensing and Wnt signaling. Bone, 2008. **42**(4): p. 606-615.

117. Gao, Q., et al., Effects of global or targeted deletion of the EP4 receptor on the response of osteoblasts to prostaglandin in vitro and on bone histomorphometry in aged mice. Bone, 2009. **45**: p. 98-103.

118. Jee, W.S.S., H.Z. Ke, and X.J. Li, Long-term anabolic effects of prostaglandin-E2 on tibial diaphyseal bone in male rats. Bone and mineral, 1991. **15**(1): p. 33-55.

119. Minamizaki, T., et al., EP2 and EP4 receptors differentially mediate MAPK pathways underlying anabolic actions of prostaglandin E2 on bone formation in rat calvaria cell cultures. Bone, 2009. **44**(6): p. 1177-1185.

120. Jee, W.S.S. and Y.F. Ma, The in vivo anabolic actions of prostaglandins in bone. Bone, 1997. **21**(4): p. 297-304.

121. Gao, Q., et al., Effects of prostaglandin E2 on bone in mice in vivo. Prostaglandins and Other Lipid Mediators, 2009. **89**(1-2): p. 20-25.

122. Hughes-Fulford, M., Signal transduction and mechanical stress. Science's STKE [electronic resource] : signal transduction knowledge environment, 2004. **2004**(249).

123. Zhao, S., et al., MLO-Y4 osteocyte-like cells support osteoclast formation and activation. Journal of bone and mineral research, 2002. **17**(11): p. 2068-2079.

124. Silvestrini, G., et al., Detection of osteoprotegerin (OPG) and its ligand (RANKL) mRNA and protein in femur and tibia of the rat. Journal of Molecular Histology, 2005. **36**(1-2): p. 59-67.

125. Glass Ii, D.A., et al., Canonical Wnt signaling in differentiated osteoblasts controls osteoclast differentiation. Developmental Cell, 2005. **8**(5): p. 751-764.

126. Tan, S.D., et al., Fluid shear stress inhibits TNF alpha-induced osteocyte apoptosis. Journal of Dental Research, 2006. **85**(10): p. 905-909.

127. Kitase, Y., M.L. Johnson, and L.F. Bonewald, The protective effects of mechanical strain on osteocyte viability is mediated by the effects of prostaglandin on the cAMP/PKA and the beta-catenin pathways. Journal of bone and mineral research, 2007. **22**: p. S178-S179.

128. Bhalla, S., et al., β_1-integrin mediates pressure-stimulated phagocytosis. American Journal of Surgery, 2009. **198**(5): p. 611-616.

129. Craig, D.H., et al., Increased extracellular pressure enhances cancer cell integrin-binding affinity through phosphorylation of Î²₁-integrin at threonine 788/789. American Journal of Physiology - Cell Physiology, 2009. **296**(1).

130. Litzenberger, J.B., et al., Deletion of β_1 integrins from cortical osteocytes reduces load-induced bone formation. Cellular and Molecular Bioengineering, 2009. **2**(3): p. 416-424.

131. Bezooijen, R.L., et al., SOST/sclerostin, an osteocyte-derived negative regulator of bone formation. Cytokine & Growth Factor Reviews, 2005. **16**(3): p. 319-327.

132. Liu, J., et al., Hydrostatic pressure promotes Wnt10b and Wnt4 expression dependent and independent on ERK signaling in early-osteoinduced MSCs. Biochemical and Biophysical Research Communications, 2009. **379**(2): p. 505-509.

Appendix

Peer reviewed journal publications

Chao Liu, Yan Zhao, Wing-Yee Cheung, Ronak Gandhi, Liyun Wang, Lidan You "Effects of cyclic hydraulic pressure on osteocytes" Bone. Volume 46, Issue 5, May 2010, Pages 1449-1456

Jan-Hung Chen*, **Chao Liu***, Lidan You, Craig A. Simmons "Boning up on Wolff's Law: Mechanical regulation of the cells that make and maintain bone" Journal of Biomechanics 43 (2010) 108-118, *These authors made equal contribution

Accepted publications

Wing-Yee Cheung, **Chao Liu**, Craig A. Simmons, Lidan You, "Osteocyte Apoptosis is Mechanically Regulated and Induces Angiogenesis In Vitro", (2010), Journal of Orthopedic Research

Conference activities

June 2010	16th Canadian Connective Tissue Conference	Toronto, ON, Canada	Oral presentation
Mar. 2010	Orthopaedic Research Society 56th annual meeting	New Orleans, Louisiana, USA	Poster presentation
Oct. 2009	2009 Biomedical Engineering Society Annual Meeting	Pittsburgh, PA, USA	Oral presentation
Sept. 2009	10th International Bone Fluid Flow Workshop	Hershey, PA, USA	Oral presentation

Feb. 2009	Orthopaedic Research Society 55th annual meeting	Las Vegas, Nevada, USA	Poster presentation